Strengthening of Timber Beams with High strength steel cords

A Borri, M Corradi[1]

Civil and Environmental Engineering Department, University of Perugia,

Via Duranti 92 06125, Perugia, Italy

ABSTRACT:

This paper presents an experimental study on the strengthening of wood beams under bending loads through the use of very high strength steel cords. The study also presents the results of 21 double shear push-out tests conducted to determine the strength of Steel fiber Reinforced Polymers (SRP) bonded to wood prisms. An experimental programme based on a four-point bending test configuration is proposed to characterize the stiffness, ductility and strength response of strengthened wood beams. Mechanical tests on the strengthened wood showed that external bonding of steel fibers produce high increases in flexural stiffness and capacity. Finally experiment results are used to calibrate existing analytical formulations for capacity prediction. This economic and effective technique may be an interesting alternative to glass or carbon fibres or other expensive retrofitting methods.

Keywords: A. Fibres, A. Wood, B. Adhesion, B. strength, D. Mechanical testing.

1. INTRODUCTION

Considering the deteriorating state of the infrastructure worldwide (bridges, buildings, etc.) and the limited resources available for repair and rehabilitation of constructed facilities, it is important to find effective and economic methods in order to maintain in use these structures. The use of metal elements in order to reinforce wood members is not new. Steel bars have been used as glulam strengthening by

[1] Corresponding Author: mcorradi@strutture.unipg.it, tel +39 075 585 3906 fax +39 075 585 3897 (M. Corradi).

Dziuba [1] and Bulleit et al. [2]. Steel and aluminium plates have been placed between laminations both vertically and horizontally by Borgin et al. [3], Stern and Kumar [4], Coleman and Hurst [5]. High strength steel wire embedded in an epoxy matrix has been used to replace tension laminations of wood beams by Krueger et al. [6,7], Kropf and Meierhofer [8]. However, most of these techniques have never been used to consolidate existent or old wood beams where it is not possible, for various reasons, to carry out a complete replacement of the wood element. Seismic or static upgrading works are often necessary for existing wood members and external bonding of strengthening is a possible solution.

Thanks to the notable advances registered in the academic, as well as industrial research sectors over the last years, the use of advanced materials and techniques has become more and more frequent in the field of civil engineering. This situation has led to a better understanding of these materials as well as of the applicative technologies involved. This has been particularly true for fiber-reinforced composites, FRP (*Fiber Reinforced Polymers),* introduced following the Second World War and which originally found use in the military and in aerospace projects for their mechanical properties and light weight.

Their use in the field of construction goes back to the beginning of the 1990s when they were utilized as strengthening in pre-existing reinforced concrete structures. It was only later that their use was extended to the areas of masonry, wood and steel structures.

Although wood structures have played an important role in construction, they have acquired a reputation for impermanence and limited application. The strengthening of wooden beams using composite materials is designed to enhance both the capacity as well as the flexural stiffness. Similar upgrading works are defined as “global” since they regard the whole structure, while the term “local” is used to define those applications involving a strengthening concentrated in a particular area (shear strengthening, reconstruction of beam headpieces and joint restoration).

A consolidation of the “global” type may be held necessary for a variety of reasons. The most common among these are due to accidental load variations common to historic structures, decreases of the resistant sections following degradation (attacks by biological agents such as insects, fungus, etc.) or following non-biological events such as blows, fire, or cracks due to a differentiated shrinkage of the wood.

At this time there is an ample bibliography of the experimental research carried out on the use of FRP composite materials in the strengthening of wood elements, highlighting the effectiveness of this consolidation technique. Among those that can be cited are those carried out by Plevris and Triantafillou

[9] and by Triantafillou [10] dealing with external carbon strengthening (CFRP) in the presence of flexure and shear loads on small dimension samples; by Johns and Lacroix [11] on samples 39x89x1675 mm, strengthened with various FRP patterns; by Borri et al. [12, 13] on wood beams strengthened using CFRP sheets and bars; by Gentile et al. [14], by Fiorelli and Alves Dias [15], Alam et al. [16].

Research in the field of composite materials not only leads to improved mechanical performance but also to a steady decrease in the costs of production and mounting, which perhaps up to now have represented the major obstacles to their utilization. In addition to costs however, another point of FRP materials is that of being extremely anisotropic. An important characteristic of these materials is their elevated tensile strength in the direction of the fibers, while evidencing extremely low resistance in all other directions. Moreover, some FRP materials demonstrate significant diminutions in strength and elastic modulus with environmental aging or following water absorption (Prian and Barkatt, [17]) (Liao et al., [18]).

A partial solution to the above problems can be found with the use of *Steel Reinforced Composites*, a new type of composite material with the particularity of being constituted of metallic fibers realized with very high strength small steel filaments. These are wound in a spiral to form cords and embedded in a matrix of either thermo-plastic or epoxy polymer (SRP: *Steel Reinforced Polymer*) or cement (SRG: *Steel Reinforced Grout*). But, why is a steel strengthening preferred over glass or carbon fibre? SRPs have multiple advantages: first of all, the use of metallic cords - which can be compared to carbon or glass fibers in terms of strength - offers lower production costs, a ductility intrinsic to steel, some resistance to flexure and, above all, to shear, which results in their wider possible application as opposed to traditional carbon or glass fibers. This is particularly important for a wood beam strengthening: beam failure is usually caused by tensile wood fracture provoking out of plane and shear loads in the strengthening materials. SRP are also much more economic compared to carbon or glass fibers, their LCA (Life Cycle Analysis) is significantly less energy consumer [19].

It has to be noted that, even if the basic idea proposed here is similar to FRP materials, the use of SRPs presents advantages and disadvantages which were not studied before. Their bond properties with resins, their significant bending stiffness and their macrostructure are different compared to FRPs. The use of steel fibers characterised by a lower modulus of elasticity may avoid stress concentration and premature fiber or wood ruptures. Among the disadvantages of these new steel fibers must be noted the oxidation that metal sheets are subject to. However, the coupling of these with epoxy resins which completely

surround the sheets, blocking water infiltration and thereby preventing the process of oxidation, can solve the problem.

2. MECHANICAL PROPERTIES OF THE MATERIALS

2.1 *Description of the strengthening*

All the cords are made up of high strength steel filaments covered with a layer of brass to prevent oxidation and increase bonding with the matrix. The typologies of used cords are shown in figure 1, each identified by name. Placing these metallic cords side-by-side and gluing them onto thin polyester meshes results in a product in the form of sheets of varying cord/cm densities (4, 12 and 23 cords/inch corresponding to, respectively, 1.57, 4.72 and 9.05 cords/cm), which are then wound on bobbins (Fig. 2). Two types of cords have been used for the present experiment (commercial names 3X2 (cord A) and 3SX (cord B)).

2.1.1 Cord A

The cord A results from the winding of five single high strength filaments in a helix: two filaments are wound around three internal filaments. Table 1 shows the geometric and mechanical properties of a single cord. The mono-directional sheet used in the experiment was the medium density (tape weight 1.80 kg/m^2). Mechanical properties of cord A were verified by tensile tests carried out on 8 samples. The results substantially confirmed the values reported by the manufacturer in its technical sheet, with variations in the order of 10%: failure load 1383 N (technical sheet 1539 N), deformation at failure 2.2% (technical sheet 2.1%).

2.1.2 Cord B

The cord B results from winding four single high strength metallic filaments together: three filaments are wound together by a single external filament of smaller diameter. The geometric and mechanical properties of a single cord are shown in Table 1. As for the cord A, three different sheet types - depending on 3 different cord densities- are currently in use. The medium density mono-directional sheet (4.72 wire/cm, 2.11 kg/m^2) was used for strengthening. Cord B mechanical properties were verified by means of a series of tensile tests. These tests carried out on 7 samples again substantially confirmed the technical

data furnished by the manufacturer. In particular an average failure load of 1407 N and a corresponding deformation of 2.5% resulting from the tests were compared with declared values of, respectively, 1343 N and 2.3%.

2.2 *Description of structural adhesives*

Two types of polymer resin were utilized to glue the steel cords to the tension area of wood beams and rafters. Although both are epoxy systems, one is a resin characterized by an elevated glass transition temperature and thus maintains its mechanical properties even at high temperatures.

2.2.1 *Resin No. 1*

This is an epoxy system composed of a bi-component thixotropic adhesive based on an epoxy resin without solvents, available under the brand name Kimitech EP-TX. It offers good adhesion to various supports and does not shrink while hardening. The properties of this epoxy system as declared by the producer appear in Table 2.

2.2.2 *Resin No. 2*

This is a thixotropic bi-component epoxy system without solvents. It is produced and marketed by Elantas Camattini under the brand name AS 90/AW 09. Hardens well even under conditions of high humidity, it offers resilient gluings. The main properties of the resin, hardener and of the whole epoxy system shown in the product technical sheet are summarized in Table 2.

2.3 *Wood elements*

The purpose of the experimental work was to investigate the effectiveness of strengthening with steel fibers glued to the tension area of wood elements, using the polymeric (epoxy) resins described in section 2.2. To this end, 24 wood rafters and 13 beams were prepared: rafters of white fir wood (*Abies alba*), nominal dimensions 100x100x2000 mm; 13 beams, nominal dimensions 200x200x4000 mm, of which 6 in oak (*Quercus sessiliflora*) and 7 in white fir wood (*Abies alba*). All samples had sharp corners, were certified to be of seasoned timber, and were characterized by an average moisture content: 10.6 % for the rafters 11.5 % for the oak beams, and 12.3 % for those of fir wood.

In accordance with standard UNI 11035 [20], fir wood structural elements are distinguishable, per visual examination, into three resistance categories: S1, S2 and S3. Even if visual grading can have a lack of reliability, each element was assigned to one of the three categories in accordance with the rules determined by the second part of standard UNI 11035 [21]. Based on these analyses, the weight density of the 24 rafters was 423 kg/m^3 , while they were spread over the resistance classes with 4 in S1 (specimen No. R3, R9, R14 and R16), 16 in S2 and 4 in S3 (R12, R18, R21 and R23) (Fig. 3). The 7 fir wood beams were classified in S1 (Fir No. 9, 11, 12, 13) and S2 (Fir No. 7, 8, 10) with a weight density of 465 kg/m^3. The oak beams were all classified in category S in accordance with the same standard and had a weight density of 796 kg/m^3.

Wood specimens cut from rafters and beams were tested in traction and compression according to ISO 3345 [22] and ISO 3787 [23] standards. Results for wood strengths and Young modulus are reported in Table 3. The theoretical model stabiles that the timber presents an elastic-plastic behavior in parallel compression. The relation among the plastic strain and elastic strain was determined experimentally with compression tests using small size simple of dimensions (20×20×60 mm) and deflection velocity of 0.002 mm/min.

3. EXPERIMENTAL ANALYSIS

3.1 Bond tests

The bond test performed provided a shear force at the interface SRP sheet-wood. The bonding test is a type of double lap shear test, for which the strengthening sheet was bonded onto two opposite sides of two wood prism. In fact the test specimens were built by bonding two symmetrically located SRP laminates along the center line of two similar wood prisms. Each specimen was made in fir wood and was inserted into a steel box fixed at the bottom grip of the testing machine. The free end portions of the sheet were fixed at the opposite side, once a special gripping device was provided, therefore a tensile force was applied. Figure 4 illustrates the test set-up and is self explanatory. The tests were carried out under displacement control, with a displacement rate of 0.2 mm/min. Different bond lengths, L = 30, 40, 50, 75, 100 and 150 mm, were utilized. Special attention was given to eliminate any possible eccentricities on SRP laminates that could cause premature failures. Displacements were continuously monitored using

two LVDTs that were located at the outer edges of the blocks. The data were collected automatically using a computerized data acquisition system.

Prior to application of the SRPs, surfaces of wood were cleaned from dust by air-blowing. Then, SRP sheets, cut to predetermined length and width (20 mm, 10 cords), were impregnated into the epoxy resin No. 1 and bonded on the sides of the wood blocks. All the tests were performed after seven days of SRP application for a uniform amount of curing time.

3.1.1 Test results

The results obtained from experiments conducted on 21 double shear specimens are presented in this section. Hence, the statistical variability in bond strength due to specimen manufacturing and testing was not investigated. On the other had, the aim of the tests was to investigate strength variability as a function of the bond length. In this regard, special attention should be paid in interpreting the results. However, the experiments are believed to provide information on the expected trends of bond strength when different bond lengths are employed. The results presented below are examined in the sense of demonstrating expected order of magnitude for bond strength and variation of it with test parameters.

The summary of experimental results including ultimate loads, normalized strength (P_{test}/P_{SRP} where P_{SRP} is the uniaxial tensile strength of bonded SRP sheet) and failure modes are summarized in Tables 4 and 5. Pictures of the specimens for different failure modes are given in Figure 5.

Results showed that with increasing bonded length, L_{SRP}, load carrying capacity increased up to a certain length beyond which no strength enhancement occurs. This length, generally referred as the effective bond length was found to be about 100 mm for a wood compression strength of 34.3 MPa. The corresponding maximum strength was found as 70-75% of the uniaxial load carrying capacity of the SRPs.

From tests, it was evident that increase in bonded length of the SRP laminates resulted in a decrease of normalized strength. The failure mode for all specimens with bonding lengths of 30-50 mm was debonding of the SRP from the wood surface or cord pull-out from epoxy resin. The bond strength is found to be extremely sensitive to anchorage length. By increasing the bond length up to effective bond length, load carrying capacity of the anchor increased significantly.

Post-failure examinations were carried out on selected test specimens using a scanning electron microscope (SEM) to study the adhesion and failure mechanisms of the composite. It is evident from Figure 6 that the wettability of the epoxy resin is not high. The figure suggest that the wettability of the epoxy resin on cords could be increased by using low cord-densities or appropriate cord coatings.

3.2 Bending tests

The wood beams and rafters underwent a four-point bending test with a constant moment region in the middle third of span. The midspan and loading point deflections were recorded using inductive four transducers (LVDTs). A data acquisition system for an instrumentation board (Catmodule ver. 8.0) of 6 channels was used to record load, deflections and time readings.

In the case of the rafters, the simply supported span between the two bearings, made of two semi-cylindrical metal elements (diameter 609 mm), was 1900 mm. The load span was equal to 640 mm. The rafters were loaded with a 245kN MTS actuator and a spreader beam. The spreader beam, centered about the midspan, created a 640 mm zone with constant moment and zero shear. The wood rafters were strengthened with metal cords (types A and B) utilizing sheets 1850x50 mm or 1850x100 mm (Fig. 7). In order to prevent strengthening detachment, two wood rafters (R5 and R13) were reinforced with steel cords glued to wood surface with an epoxy resin and two metal plates (dimensions 90x50x2 mm) fixed with eight screws at both sheet ends.

The tests on the oak and fir wood beams were carried out on a clear span of 3900 mm and a load span of 1300 mm (Fig. 8). The strengthenings, 70x3800 mm or 140x3800 mm, were placed centrally in the tension zone. Beams nos. 2, 3, 7 and 13 were strengthened with a SRP strip, (cord A, 70x3800 mm) glued on a continuum in the wood tension zone. Beams no. 6, 9 and 10 instead, were strengthened with cord A sheets 140 mm wide. In the case of cord B, strengthenings 70 mm wide were applied to beams nos. 4 and 8, while strengthening of 140 mm width was applied to beam nos. 5.

Beam no. 3 was strengthened with a SRP strip (cord A, width 70 mm) positioned similarly, however glued at the strip ends and fastened with a 120 Nmm coupling by means of a mechanical device, consisting of a metal cylinder, positioned at one end. Figure 9 shows the device utilized for pre-tensioning of the steel cords. This is composed principally of a metal cylinder, around which the cords are wound.

Once the strip is fastened to the other end with a clamp, (Fig. 10) into which an epoxy resin is injected, the metal cord is wound around the metal cylinder until a determined clamping couple results. The final result is a wood beam strengthened in the tension zone with pre-tensioned steel cords fixed with two clamps at beam ends.

The results presented here are in terms of the ultimate load carrying capacity of beams or rafters. In addition, the results include investigating the deformational properties of the strengthened and unstrengthened beams in terms of the load-deflection relationship and ductility.

Rafters and beams were tested under two monotonically increasing concentrated loads applied at 1/3 and 2/3 of span of the wood elements using displacement-control mode at a loading rate of approximately 5 mm/min. At the end of the test measurements were taken of the load history, maximum load P_{max} , and deflections of some points using inductive transducers. Two equivalent flexural stiffnesses, $k_{1/3}$ and k_{ult}, were then calculated:

$$k_{1/3} = \frac{0.33 P_{\max}}{f_{1/3}}; \tag{1}$$

$$k_{ult} = \frac{P_{\max}}{f_{\max}} \tag{2}$$

where $f_{1/3}$ and f_{max} are the midspan deflections corresponding to 33% and 100% of the maximum load P_{max}.

3.2.1 Non-strengthened elements (rafters and beams)

Three of the thirteen beams and four of the twenty-four rafters were used as controls and underwent testing without any prior strengthening. The sole purpose was to investigate the stiffness, ductility and flexure capacity of such elements without strengthening and, by an opportune comparison of the results, be able to analyze the effectiveness of the various strengthening t techniques experimented.

The test results for the unstrengthened elements demonstrate a quasi-linear-elastic behaviour up to failure, which presented in the wood tension zone starting from a knot or a defect. Wood without defects has a high compression and a very high tensile strength parallel to the timber's grain, but defects like knots reduce tensile/bending strength much more then the compression strength. Low quality woods present very low tensile strength and this prevent yielding of wood in compression.

A slight loss of stiffness, more evident for rafters nos. 22 and 24, was probably the result of a premature partial rupture and not due to yielding in the compressed zone. From the results obtained, even though scattered, it was possible to have information about the flexural strength and stiffness of both the rafters and the beams.

An average failure load of 14.2 kN and a stiffness $k_{1/3}$ of 0.395 kN/mm were measured for the rafters. Similarly to the case of the rafters, one unstrengthened beam in oak and two in fir wood were tested in order to measure their capacity and flexural stiffness. The oak beam broke at a load of 63.4 kN demonstrating a flexural stiffness of 1.109 kN/mm, calculated according to (1). The fir wood beams demonstrated a lower average flexural stiffness of 0.95 kN/mm, while in the case of the flexural resistance they broke at an average load of 58.1 kN. The observed mode of failure of un strengthened beams was always due to cracking of the timber (tension failure) from a knot or a defect.

3.2.2 Strengthened elements

3.2.2.1 Rafters

A total number of twenty wood rafters and ten wood beams was strengthened with high strength steel cords. Tables 6 reports the comparison between the average stiffnesses $k_{1/3}$ and k_{ult} and failure loads for strengthened and unstrengthened samples. Even if tensile strength of 3X2 and 3SX cords is significantly different (respectively 2479 MPa and 1657 MPa), their tensile failure load is similar (respectively 1539 N and 1343 N for a single cord). As a consequence, results of rafters and beams strengthened with cords A and B of the same width are not significantly different, even though caution must be used in light of the limited statistical sample.

A minimum increase of capacity of 38 percent was measured for rafters strengthened with 70 mm wide sheet (cord A, resin No. 1), while the maximum increase value (77 percent) was recorded for rafters strengthened with 100 mm wide sheet (cord B, resin No. 1).

A second consequence of the strengthening is the increase of the stiffness $k_{1/3}$ of the rafters. The maximum increase value is 49 percent and the average value is 30 percent. The strengthening t also caused an increase in ductility of rafters. The values of $k_{1/3}/k_{ult}$ highlight that the behaviour of un strengthened rafters is quasi-linear ($k_{1/3}/k_{ult}$=1.19), while for strengthened rafters $k_{1/3}/k_{ult}$ reached the value of 1.63.

Failure of the strengthened wood rafters occurs in different ways (Tab. 6). However, in most cases fracture originates in the wood in the tension area (usually initiating with a defect in the wood) and subsequently causes a failure by tension in the steel cords or a partial detachment of the strengthening. The graph in Figure 11 represents the comparison between test results for the unstrengthened rafters and those strengthened with a 100 mm wide (cord A). Another graph is reported in Figure 12: it compares the unstrengthened rafters and those strengthened with a 50 mm wide strip (cord A).

Also reported are in Table 6 the results obtained for the rafters strengthened with cords A, on which metal plates were placed at the ends of the 50 mm wide strengthening. The two rafters tested exhibited an average failure mode of 24.1 kN and a stiffness $k_{1/3}$ of 0.587 kN/mm. Although the application of the plates did not have a notable effect on stiffness, it positively acted to prevent strengthening detachment.

3.2.2.2 Beams

The results of the tests on the six oak beams also evidence significant increases in capacity, confirming those obtained for the wood rafters. In particular, while the unstrengthened oak beam failed at a flexural load of 63.4 kN, the two beams strengthened by gluing a 70 mm wide strengthening in the tension area failed at an average load of 119.5 kN, for an increase of approximately 88 percent. Strengthening by the gluing on of metal cords resulted in a 34 and 87 percent average increase respectively in flexural stiffnesses $k_{1/3}$ and k_{ult} (Fig. 13 and Tab. 7). The failure of the strengthened wood beams has its beginning at a point in the tension zone of the wood itself. In particular, fracture in the oak beams strengthened by the gluing on of metal cords occurs in that part of the tension zone not covered by the strengthening (therefore at the edges of the beams). In the areas where the sheet is glued on to the beam using an epoxy resin there is a positive “blocking” action of the cracks which propagate out from defects present in the wood itself (grain deviation, knots, cracks due to shrinkage). The load–deflection curve for the strengthened fir wood beams is shown in Figure 14.

Strengthening by means of pre-stressed cords does not increase flexural strength compared to that carried out by means of continuous reinforcement gluing. In this latter case only a 38 percent increase in capacity was noted. This strengthening technique did not cause the positive defect-blocking action described above. In addition the steel cords are not embedded (and therefore protected) into the epoxy resin.

Finally the test results for the fir wood beams highlight similar increases in capacity compared to those for oak beams. The beams strengthened with 70 mm wide SRP sheets failed at an average load of 74.3 kN, for a 28 percent increase relative to those unstrengthened, while those strengthened with 140 mm wide sheet broke at a load of 88.1 kN for a relative increase of 52 percent.

The strengthening, placed in the tension zone, never debonded from the wood surface and the tension failure of wood caused the reinforcement fracture (Fig. 15). Strengthening results more effective in those wood beams of lower quality (fir-wood) which demonstrate plastic behaviour under compression only when strengthened. This is the case of those wood beams with defects, above all in the tension area. The yield of the compressed zone results in flexural plastic behavior. In this way it is possible to activate the tensile strength of the strengthening which determines improved reinforcement effectiveness. The graphs in Figures 13 and 14 represent a comparison between the load–deflection curves of strengthened and unstrengthened beams respectively for fir and oak wood beams. We can observe that the behavior of strengthened beams is often different from that of unstrengthened one. The strengthening has caused an increase in ductility ($k_{1/3}$/ k_{ult}) of the most part of strengthened beams.

4. ANALYSIS OF THE RESULTS

In this work it is assumed a concept that was presented by Buchanan [24, 25] where the timber, when submitted to tensile efforts, presents an elastic-linear behavior, and when submitted to compression efforts the timber presents an elastic-linear behavior and a nonlinear inelastic behavior.

In particular, the law for the wood can be expressed by (assuming the compression and tensile elastic moduli $E_{Wc} \cong E_{Wt} = E_W$) (Fig. 16):

$$\begin{aligned} &\sigma_{Wc} = E_W \cdot \varepsilon_{Wc} && \text{if} \quad \varepsilon_{Wc} < \varepsilon_{Wc0} \\ &\sigma_{Wc} = \sigma_{Wc0} && \text{if} \quad \varepsilon_{Wc} > \varepsilon_{Wc0} \\ &\sigma_{Wt} = E_W \cdot \varepsilon_{Wt} \end{aligned} \tag{3}$$

σ_{Wc} and σ_{Wt} are respectively the wood compression and tensile stress parallel to the timber's grain, E_W is the wood Young modulus, ε_{Wc} and ε_{Wt} are the wood strains in compression and in tension. ε_{Wc0} is the strain value at yield stress $\sigma_{Wc0.}$

With regard to steel cords the generic stress-strain relationship will assume the following expressions:

$$\sigma_f = E_f \cdot \varepsilon_f \tag{4}$$

The non-linearity observed for strengthened rafters/beams is the consequence of yielding of wood in compression.

The development of a calculation model that determines the value of the ultimate bending strength of strengthened timber beams is crucial to the material's correct and safe use in structural strengthenings and repairs, as well as to its broader use in civil construction. In order to determine the ultimate bending moment, some authors have developed for FRP reinforcements (Triantafillou and Deskovic, [26]), (Lindenberg, [27]), (Fiorelli and Alves Dias, [15]) theoretical models based on the of hypothesis of Navier/Bernoulli (plane sections remain plane after being strained) and considers the limit states of the timber's tension and compression failure.

The timber's tensile limit state is considered to have been attained when the maximum tensile stress is equal to its tensile strength. Based on the relations established between the stresses and the strains, Figure 17 illustrates the distribution of stresses when this limit state is attained, as well as the forces resulting from these stresses and their positions. Based on the relations established between the stresses and the strains and on the condition of equilibrium of forces, we have:

$$F_I + F_{II} = F_{III} + F_{IV} \tag{5}$$

where the forces in the compression region are given by:

$$F_I = \sigma_{Wc0} \cdot b \cdot \left[y - \alpha(h - y) \right]; \tag{6}$$

$$F_{II} = \frac{\sigma_{Wc0}}{2} \cdot b \cdot \alpha(h - y); \tag{7}$$

and the forces F_{III} and F_{IV} in the tension zone are given by:

$$F_{III} = \frac{\varepsilon_{Wtu}}{2} \cdot E_W (h - y) \cdot b\,; \tag{8}$$

$$F_{IV} = \varepsilon_{Wtu} \cdot E_f A_f \tag{9}$$

where:

$$\alpha = \frac{\sigma_{Wc\cdot 0}}{E_W \varepsilon_{Wtu}} \tag{10}$$

h and b are the dimensions of the cross section and ε_{Wtu} is the ultimate wood strain value in tension.

From equation (5) and from the stress-strain laws of materials it is possible to find the position y of the neutral axis. The equations in (3) do not take into account the possibility of having different wood elastic modules in tension and compression zones of the section. In effect, preceding studies on the material indicate that in an overwhelming number of cases the difference between the two modules is almost negligible, respect to other simplifications assumed.

Once the neutral axis position is found, it is possible to proceed to the calculation of the ultimate bending modulus of the section and maximum capacity of strengthened and unstrengthened wood beams.

The results presented in Table 8 were obtained both experimentally and theoretically, based on the theoretical model presented earlier herein. The theoretical values of the failure moment were determined by failure tensile, more critic situation. Table 8 presents a good relation among experimental and theoretical values. These results indicate the validated of the theoretical model. With regard to unstrengthened wood beams, the capacity determined experimentally was always lower than the numerical results while higher values of capacity were measured experimentally for almost all strengthened beams. This seems to confirm the presence of the “blocking” action of the cracks caused by the application of the steel strengthening. This action leads to an increase in the beam capacity.

5. CONCLUSIONS

The effectiveness of using high strength steel fibers for strengthening wood beams has been illustrated. There are no particular building yard problems associated with the carrying out of this type of strengthening work, which can be done within a short time without dismantling the overhanging structure.

Results of bonding tests showed that maximum strength was found as 70-75% of the uniaxial load carrying capacity of the SRPs. The bond strength is found to be extremely sensitive to anchorage length. Increasing bonded length, L_{SRP}, load carrying capacity increased up to a certain length (about 10 cm) beyond which no strength enhancement occurs.

With regard to bending tests on strengthened beams, a non-linear behavior was observed during the experimental work. This non-linearity may be due to compression yielding of the wood and/or imperfect

composite action between the wood and strengthening. However adherence between reinforcement and the wood was generally effective up to the fracture in the wood beams. The detachment of the metal cords from the wood occurred only after the fracture of the wood in the tension area. In the majority of cases failure in the wood rafters and beams was due to a fracture of the wood in the tension zone, in areas not strengthened by the metal cords.

The fracture initiated from a defect in the wood itself, such as a knot or an existing fracture due to wood shrinkage or grain deviation. The presence of steel strengthening seems to arrest crack opening, confines local rupture and bridges local defects in the timber. This causes an increase in the tensile strength parallel to the timber's grain .

In general, the behavior of the strengthened wood elements indicated significant increase in the capacity and ductility in comparison with the unstrengthened elements. Prior to yield in compression, the flexural behavior of strengthened elements was similar to that of unstrengthened ones. This behavior indicated that using steel strengthenings did not contribute significantly to increase the stiffness and strength in the elastic range. However, after wood yielding in compression, flexural stiffness and strength of the strengthened beams were improved and a more evident non-linear behavior was observed up to failure. In some cases there were increases of more than 100 percent in the maximum load when compared to the unstrengthened beams. Reinforcement turned out to be more effective for those wood beams, characterized by lower mechanical properties.

Acknowledgements

Special thanks go to dr. Roberto Nasetti, Matteo Ratini, Alessandro Bartollini and Giulio Castori. Thanks also go to Hardwire Ltd and Fidia srl for their technical assistance during the strengthening operations. The authors gratefully acknowledge the support of the Italian research project Reluis.

REFERENCES

1. Dziuba T. The ultimate strength of wooden beams with tension reinforcement. Holzforschung und Holzverwertung, 1985; 37(6):115-119.

2. Bulleit WM, Sandberg LB, Woods GJ. Steel-reinforced glued laminated timber. J. Strucl. Engrg., ASCE, 1989; 115(2):433-444.

3. Borgin KB, Loedolff GF, Saunders GR. Laminated wood beams reinforced with steel strips. J. Struct. Engrg. ASCE, 1968; 94(7):1681-1705.

4. Stern EG, Kumar VK. Flitch beams. Forest Prod. J., 1973; 23(5): 40-47.

5. Coleman GE, Hurst HT. Timber structures reinforced with light gage steel. Forest Prod. J., 1974; 24(7): 45-53.

6. Krueger GP. Ultimate strength design of reinforced timber: state of the art. Wood Sci., 1973; 6(2): 175-186.

7. Krueger GP, Eddy FM. Ultimate strength design of reinforced timber: moment-rotation characteristics. Wood Sci. 1974; 6(4):330-344.

8. Kropf FW, Meierhofer U. Strengthening, Retrofitting and Upgrading of Timber Structures with High-Strength Fibres. 2000; In: SEI 3.

9. Plevris N, Triantafillou TC. FRP reinforced wood as structural material, J. Materials in Civil Engineering, ASCE, 1992; 4(3): 300-315.

10. Triantafillou TC. Shear reinforcement of wood using FRP materials. J. Materials in Civil Engrg., ASCE, 1997; 9(2): 65-69.

11. Johns KC, Lacroix S. Composite reinforcement of timber in bending. Can. J. Civ. Eng., 2000; 27(5): 899-906.

12. Borri A, Corradi M, Grazini A, 2005. A method for flexural reinforcement of old wood beams with CFRP materials. Journal of Composites, part B, Elsevier, 36/2, p. 143-153.

13. Corradi M., Borri A. Fir and chestnut timber beams reinforced with GFRP pultruded Elements. Journal of Composites, part B, Elsevier, 2007; 38/2: 172-181.

14. Gentile C, Svecova D, Saltzberg W, Rizkalla SH. Flexural strengthening of timber beams using GFRP. In: Procedings of 3rd Int. Conf. Adv. Comp. Mat. in Bridge and Structures, 2000., Ottawa-Canada.

15. Fiorelli J, Alves Dias A. Analysis of the strength and stiffness of timber beams reinforced with carbon fiber and glass fiber, Mat. Res. 2003; vol.6 no.2, São Carlos.

16. Alam P, Ansell M. P., Smedley D. Mechanical repair of timber beams fractured in flexure using bonded-in reinforcements. Composites Part B-Engineering, 2009; 40 (2): 95-106

17. Prian L, Barkatt A. Degradation mechanism of fiber-reinforced plastics and it implications to predict of long-term bahavior, J. of mat. Science, 1999; 34: 3977-3989.

18. Liao K, Schultheisz CR, Huston DL. Effect of enivironmental aging on the properties of pultruded GFRP, Composites: Part B, Elsevier, 1999; 485-493.

19. Song YS, Youn JR, Gutowski TG. Life cycle energy analysis of fiber-reinforced composites. Composites: Part A, 2009, 40: 1257–1265

20. UNI 11035-1, 2003. Classificazione a vista di legnami italiani secondo la resistenza meccanica: terminologia e misurazione delle caratteristiche [in Italian].

21. UNI 11035-2, 2003. Regole per la classificazione a vista secondo la resistenza e i valori caratteristici per i tipi di legname strutturale italiani [in Italian].

22. ISO 3345, 1975. Wood – Test methods – Determination of ultimate tensile stress parallel to grain.

23. ISO 3787, 1976. Wood – Test methods – Determination of ultimate stress in compression parallel to the grain.

24. Buchanan AH. Combined bending and axial loading in lumber. J. Struct. Engrg., ASCE, 1986; 112(12): 2592-2609.

25. Buchanan AH. Bending strength of lumber. J. Struc. Engrg., ASCE, 116(5), p. 1213-1229.

26. Triantafillou T, Deskovic N. Prestressed FRP sheets as external reinforcement of wood members. J. of Structural Engineering, ASCE, 1990; 118 (5): 1270-1284.

27. Lindenberg RF. ReLAM: A nonlinear stochastic model for the analysis of reinforced glulam beams in bending. Ph.D. Dissertation, Dept. of Civil and Environmental Engineering, 2000; Univ. of Maine.

28. ASTM D 638-95. Standard test method for tensile properties of plastics.

29. ASTM D 790-03 Standard Test Methods for Flexural Properties of Unreinforced and Reinforced Plastics and Electrical Insulating Materials.

(a)

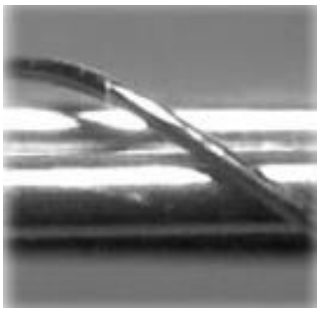

(b)

Figure 1: (a) 3X2 cord , (b) 3SX cord.

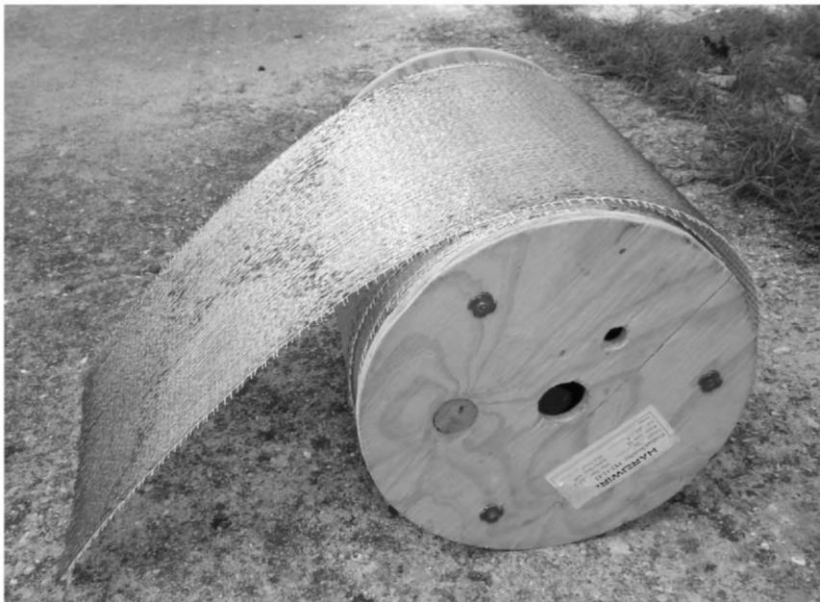

Figure 2 Steel cords.

Figure 3. Fir wood rafters.

Figure 4. Layout of bond tests.

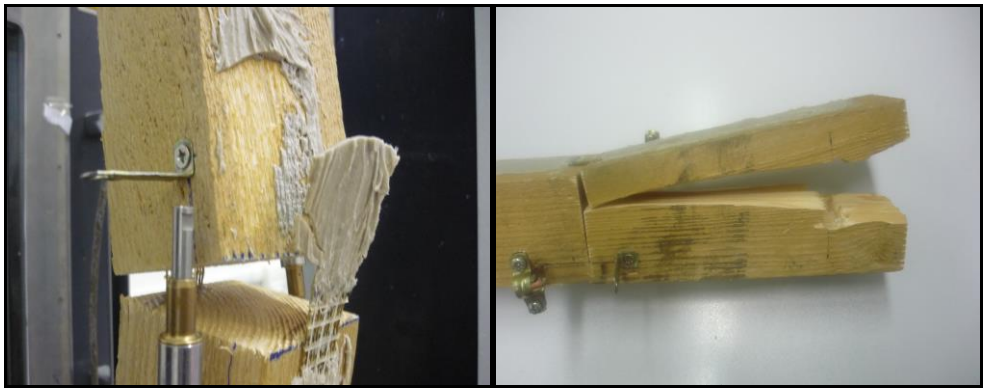

(a) Peeling (b) Wood rupture.

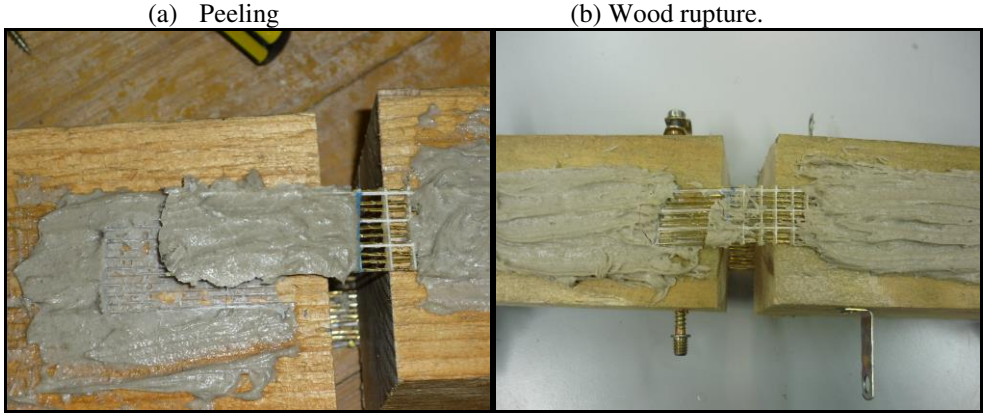

(c) Debonding (d) Cord pull-out.

Figure 5. Bond tests: failure modes.

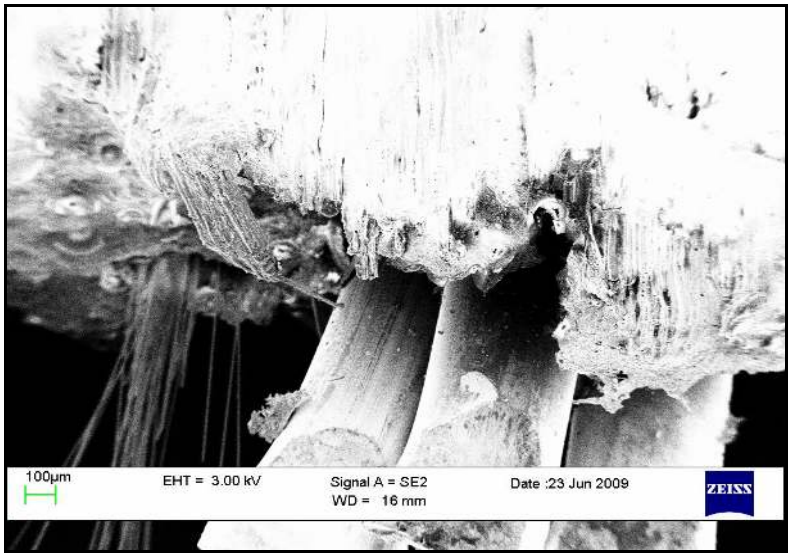

Figure 6. Electron microscopic scan (SEM) of the bond.

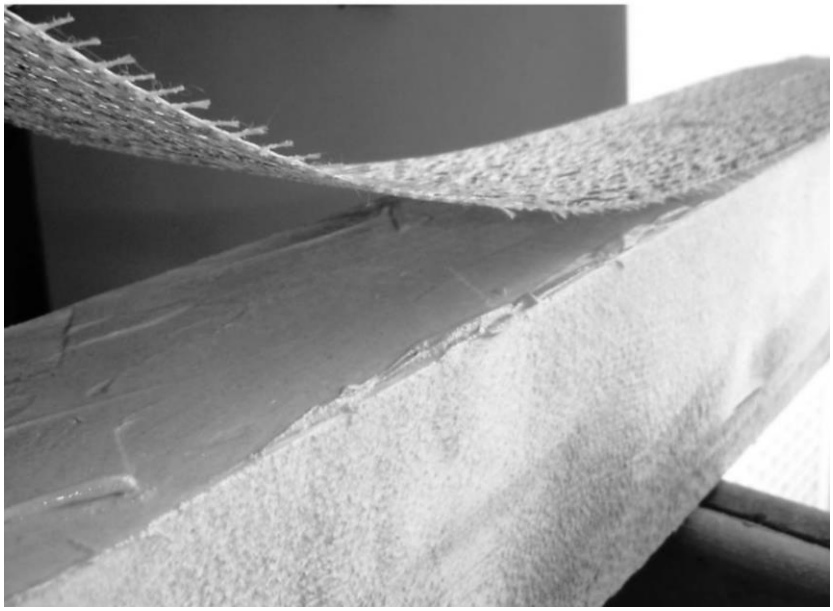

Figure 7. Application of steel cords in timber rafters.

Figure 8. Flexural test set-up.

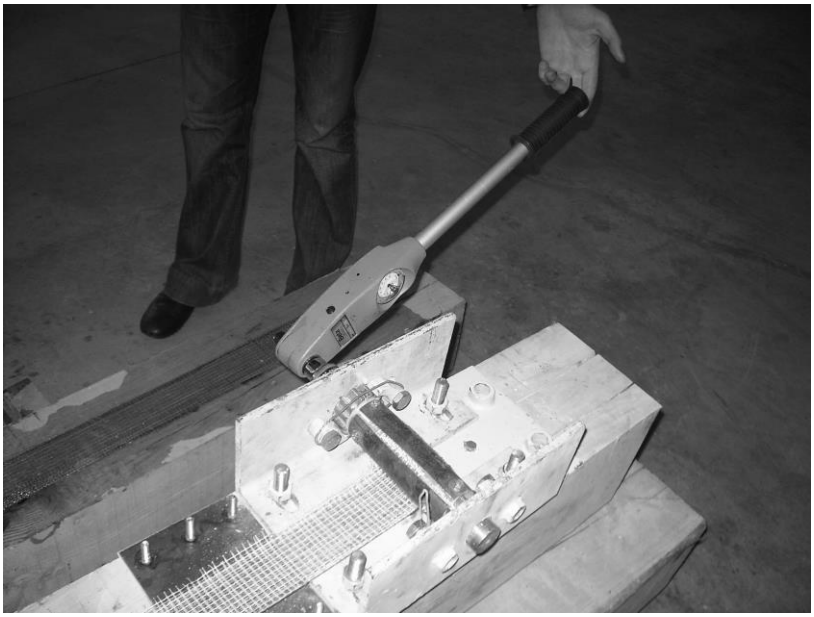

Figure 9. Prestressing technique: the metal cylinder.

Figure 10. Prestressing technique: the clamp.

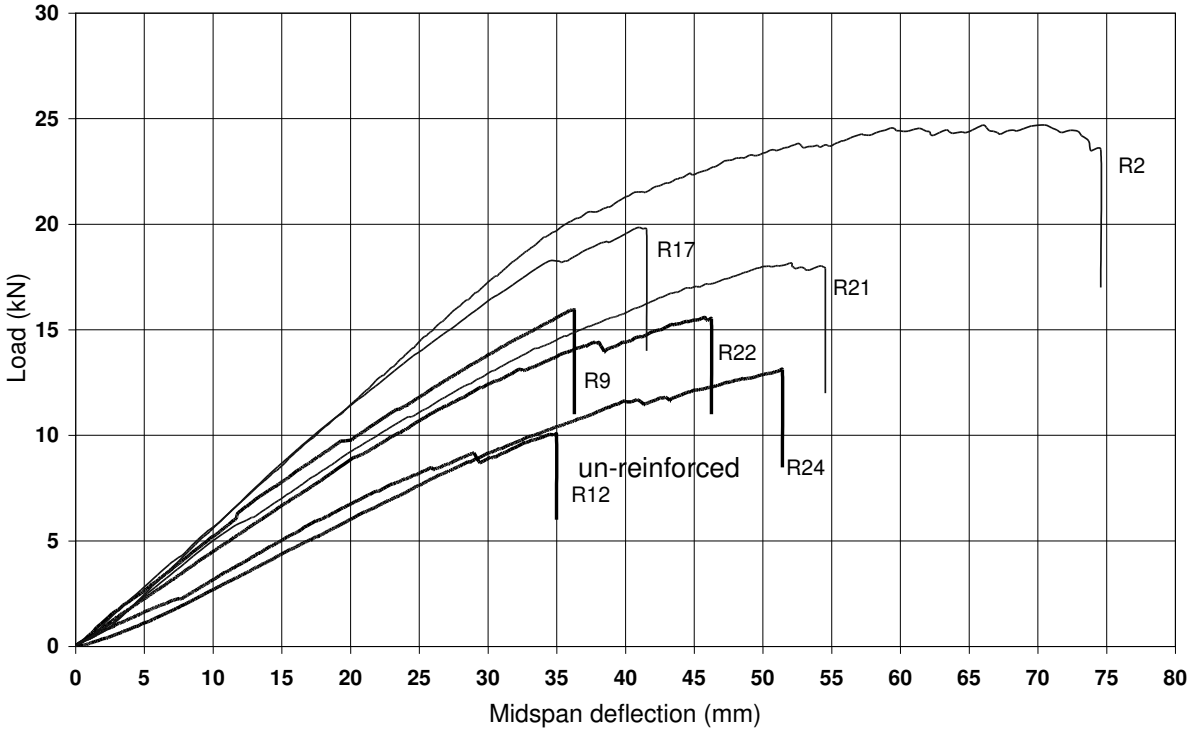

Figure 11. Ultimate static load-deflection plots for unstrengthened fir wood rafters and strengthened rafters (A-type cord width = 100 mm, resin N.2).

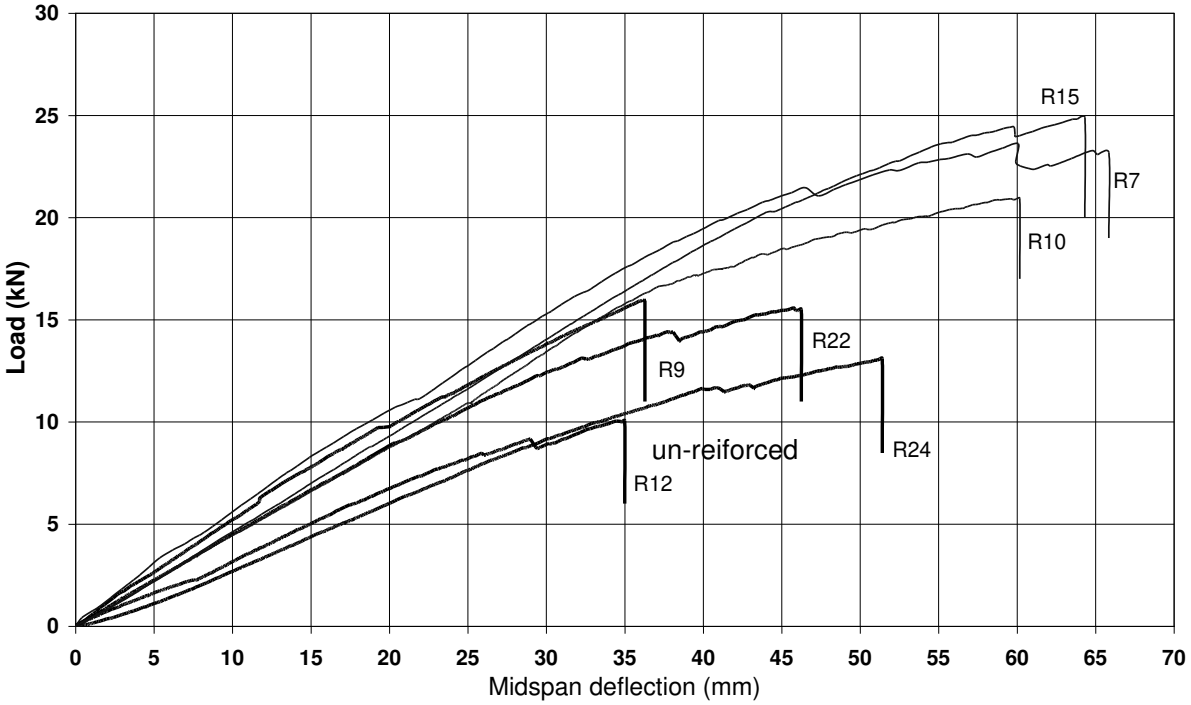

Figure 12. Ultimate static load-deflection plots for unstrengthened fir wood rafters and strengthened rafters (B-type cord width = 50 mm, resin N.1).

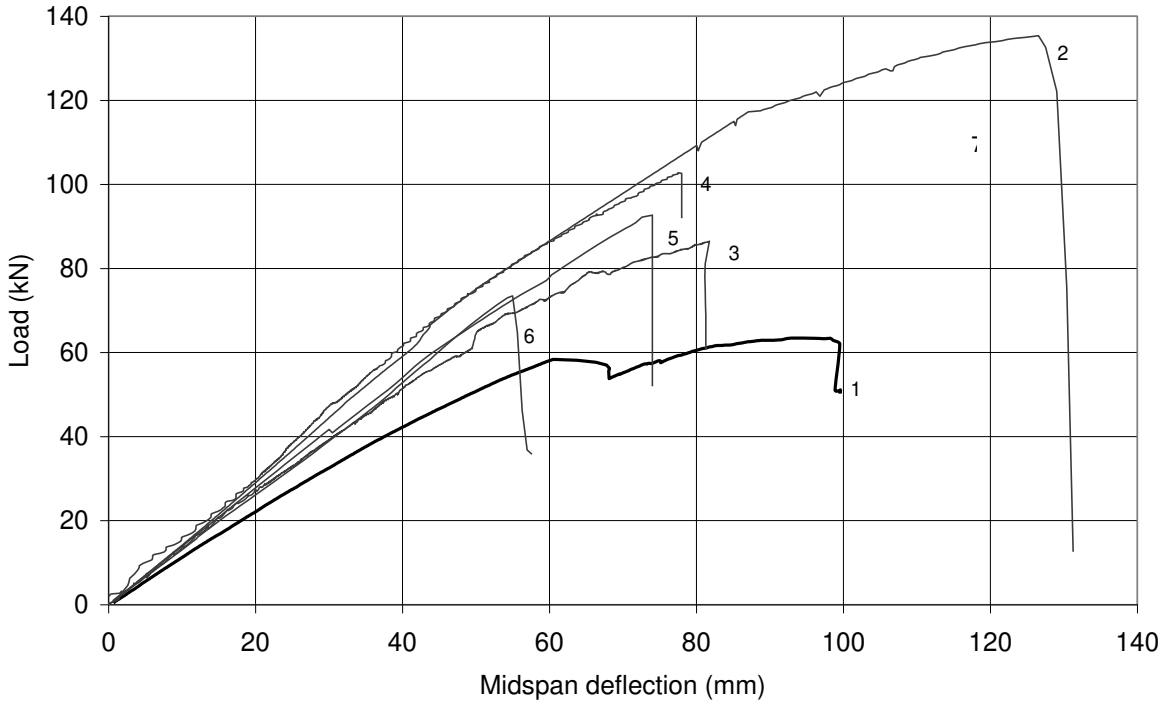

Figure 13. Ultimate static load-deflection plots for unstrengthened and strengthened oak wood beams.

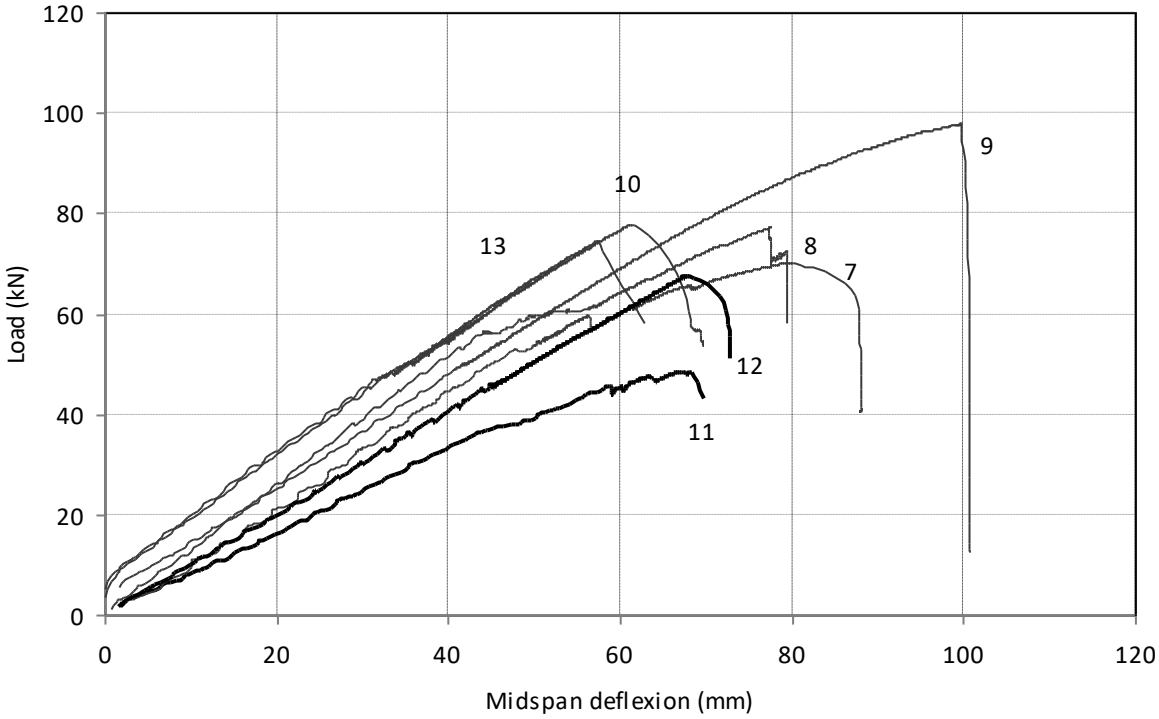

Figure 14. Ultimate static load-deflection plots for unstrengthened and strengthened fir wood beams.

Figure 15. Tension failure of wood and strengthening.

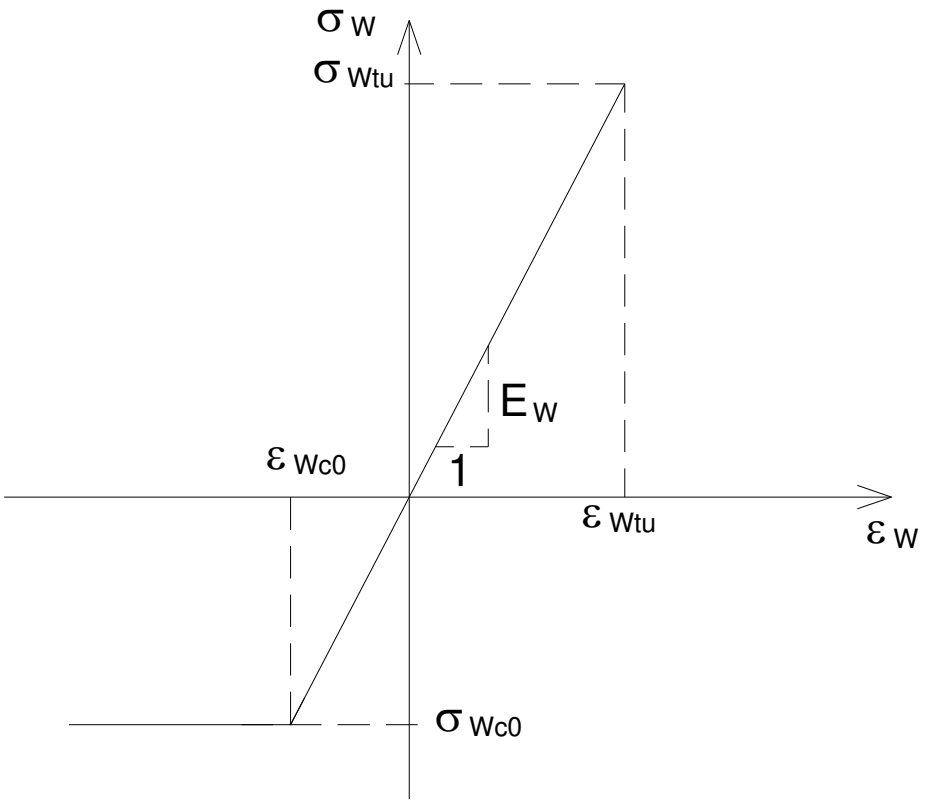

Figure 16. Used law for wood.

.

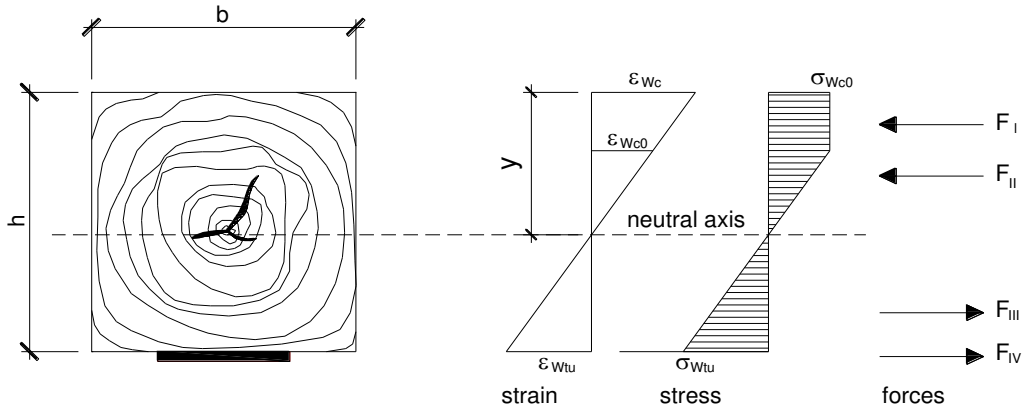

Figure 17. Distribution of strain, stress and forces in the cross section.

Table 1: Mechanical properties of high strength steel cord (commercial data).

Cord type	Cord coating	Cross Section Area (mm^2)	Failure Tensile Load (N)	Young Modulus E (N/mm^2)	Failure Stress (N/mm^2)	Diameter (mm)	Elongation At Failure (per cent)
Cord A	Brass	0.620	1539	206842	2479	0.889	2.1
Cord B	Brass	0.810	1343	206842	1657	1.016	2.3

Table 2. Mechanical properties of epoxy system [27, 28].

	Resin No. 1	Resin No. 2
Numbers of components	2	2
Full curing time at 25°C (days)	7	7
Glass transition temperature (°C)	+90	+62÷68
Resin/hardener ratio in volume	100/100	100:80
Color	Gray	White-ambra
Compression strength (MPa)	> 56	-
Flexural strength (MPa)	> 18	-
Bond strength (MPa)	2.07	-
Flexural strength (ASTM D790) (MPa)	-	35÷45
Flexural modulus (ASTM D790) (MPa)	-	1900÷2300
Tensile strength (ASTM D638) (MPa)	-	35÷45

Table 3. Results of compression and tension tests.

	Young modulus E_w (MPa)	Compression strength σ_{Wc0} (MPa)	Tensile strength σ_{Wtu} (MPa)
Oak beams	11975	34.3	50.2
Fir beams	8756	24.6	40.3

Table 4. Results of bond tests.

Bond length L_{SRP} (mm)	No. of specimens	Average ultimate load P_{test} (kN)	Failure type
30	4	9.98	Debonding/Cord pull-out
40	3	9.60	Debonding/Cord pull-out
50	5	13.3	Debonding/Cord pull-out
75	5	14.3	Wood rupture/peeling
100	2	18.9	Wood rupture/peeling
150	2	19.5	Wood rupture/peeling

Table 5. Bond tests: average bond strength and normalized strength.

Bond length L_{SRP} (mm)	No. of specimens	Bond strength (MPa)	Bond failure load P_{test}/fiber tensile failure load P_{SRP}
30	4	8.32	0.372
40	3	6.02	0.358
50	5	6.63	0.494
75	5	5.05	0.531
100	2	4.72	0.703
150	2	3.26	0.728

Table 6. Test results of fir wood rafters.

Strengthening	Specimen No.	Max load P_{max} (kN)	$k_{1/3}$ (kN/mm)	k_{ult} (kN/mm)	Failure type	$k_{1/3}/k_{ult}$	$P_{max,unreinf}/P_{max,reinf.}$
Unstrengthened	R9	16.2	0.519	0.439	a)	1.19	-
	R12	10.6	0.321	0.292	b)		
	R22	16.1	0.448	0.339	a)		
	R24	13.9	0.291	0.255	a)		
3X2, strengthening width 50 mm, resin No. 1	R4	21.2	0.563	0.434	c)	1.30	1.38
	R18	15.9	0.380	0.326	c)		
	R20	21.8	0.517	0.361	d)		
3X2, strengthening width 100 mm, resin No. 1	R3	25.9	0.638	0.315	d)	1.63	1.68
	R11	22.8	0.417	0.293	c)		
	R19	22.7	0.443	0.311	c)		
3SX, strengthening width 50 mm, resin No. 1	R7	24.0	0.555	0.393	d)	1.30	1.67
	R10	21.7	0.438	0.348	d)		
	R15	25.3	0.468	0.387	d)		
3SX, strengthening width 100 mm, resin No. 1	R8	24.4	0.471	0.364	d)	1.31	1.77
	R16	34.5	0.540	0.408	d)		
	R23	16.7	0.347	0.264	d)		
3X2, strengthening width 50 mm, resin No. 2	R1	23.0	0.480	0.353	c)	1.47	1.70
	R6	23.7	0.549	0.375	b)		
	R14	25.9	0.615	0.394	c)		
3X2, strengthening width 100 mm, resin No. 2	R2	24.7	0.572	0.350	c)	1.37	1.48
	R17	20.0	0.568	0.484	b)		
	R21	18.2	0.480	0.350	c)		
3X2, strengthening width 50 mm, resin No. 1 + metal plates	R5	24.8	0.541	0.392	d)	1.47	1.70
	R13	23.4	0.632	0.407	c)		

a) Wood tension failure. b) Wood tension failure from a knot. c) High level of wood yielding in compression, strengthening detachment. d) High level of wood yielding in compression, wood tension failure.

Table 7. Test results of oak and fir wood beams.

Specimen No.	Wood	Strengthening	Max Load P_{max} (kN)	$k_{1/3}$ (kN/mm)	k_{ult} (kN/mm)	$k_{1/3}/k_{ult}$	$P_{max,unreinf}/P_{max,reinf.}$
1	Oak	Unstrengthened	63.4	1.109	0.646	1.72	-
2	Oak	3X2, width 70 mm	135.4	1.483	1.070	1.39	2.13
3	Oak	3X2, width 70 mm*	87.7	1.342	1.072	1.25	1.38
4	Oak	3SX, width 70 mm	103.6	1.495	1.343	1.11	1.63
5	Oak	3SX, width 140 mm	92.7	1.390	1.253	1.11	1.46
6	Oak	3X2, width 140 mm	73.5	1.310	1.336	0.98	1.16
7	Fir	3X2, width 70 mm	70.8	1.164	0.890	1.31	1.22
8	Fir	3SX, width 70 mm	77.5	1.287	1.001	1.29	1.33
9	Fir	3X2 width 140 mm	98.2	1.255	0.987	1.27	1.69
10	Fir	3X2, width 140 mm	78.0	1.771	1.274	1.39	1.34
11	Fir	Unstrengthened	48.6	0.879	0.727	1.21	-
12	Fir	Unstrengthened	67.6	1.020	0.997	1.02	-
13	Fir	3X2, width 70 mm	74.7	1.856	1.303	1.42	1.29

* Pre-stressed

Table 8. Comparison with numerical results.

Wood	Reinforcement	Max Load P_{max} (kN)	Difference with numerical (%)
Oak	Unstrengthened	63.4	-32.8
Fir	Unstrengthened	58.1	-16.9
Oak	3X2, width 70 mm	111.6	14.6
Oak	3SX, width 70 mm	103.6	5.5
Oak	3SX, width 140 mm	92.7	-8.9
Oak	3X2, width 140 mm	73.5	-26.6
Fir	3X2, width 70 mm	72.8	0.1
Fir	3SX, width 70 mm	77.5	5.4
Fir	3X2 width 140 mm	88.1	16.8